Journal of Maps

ISSN: (Print) (Online) Journal homepage: https://www.tandfonline.com/loi/tjom20

Combining multi-typologies landslide susceptibility maps: a case study for the Visso area (central Italy)

Chiara Martinello, Margherita Bufalini, Chiara Cappadonia, Edoardo Rotigliano & Marco Materazzi

To cite this article: Chiara Martinello, Margherita Bufalini, Chiara Cappadonia, Edoardo Rotigliano & Marco Materazzi (2023): Combining multi-typologies landslide susceptibility maps: a case study for the Visso area (central Italy), Journal of Maps, DOI: 10.1080/17445647.2023.2198148

To link to this article: https://doi.org/10.1080/17445647.2023.2198148

JOURNAL OF MAPS
https://doi.org/10.1080/17445647.2023.2198148

Combining multi-typologies landslide susceptibility maps: a case study for the Visso area (central Italy)

Chiara Martinello [a], Margherita Bufalini [b], Chiara Cappadonia [a], Edoardo Rotigliano [a] and Marco Materazzi [b]

[a]Department of Earth and Marine Sciences, University of Palermo, Palermo, Italy; [b]School of Science and Technology, Geology Division, University of Camerino, Camerino, Italy

ABSTRACT

The research proposes a simple but geomorphologically adequate method to produce a combined landslide susceptibility map. In fact, in a logic of real use, offering type-specific landslide susceptibility maps to land use planners and administration could be not a successful solution. On the other hand, the simple grouping of more types of landslides could be misleading for model calibration considering that the relationships between slope failures and geo-environmental predictors should be conveyed by the abundance of each type of landslide resulting not specific and diagnostic for each typology. In this test, after having produced independent models for flow, slide and complex landslide by exploiting MARS (Multivariate Adaptive Regression Splines) and a set of type-specific geo-environmental variables, a combined landslide susceptibility map was obtained by combining the scores of the three source maps. The combined map was finally validated with a new unknown archive, showing very good performances.

ARTICLE HISTORY
Received 28 October 2022
Revised 22 March 2023
Accepted 27 March 2023

KEYWORDS
Landslide susceptibility; mapping units; MARS; LCL_SLU; Nera River basin (central Italy); land management

1. Introduction

One of the main issues of researchers in landslide hazard mapping, and specifically, landslide susceptibility evaluation study is to offer an easy-to-apply/-read map for the final user (land use planners and administration, Bufalini et al., 2021; Martinello et al., 2021; Smith et al., 2011). This reflects not only in the adequate partitioning of the study area, which should define mapping units geomorphologically suitable both for the modelling procedures and for obtaining final landslide susceptibility maps (Martinello et al., 2021, 2022a). In fact, considering the different typologies of landslides (Hungr et al. 2014) and the different influence of each factor in landsliding, specific modelling procedures should be analysed, and the related final maps produced. At the same time, the management of several landslide susceptibility maps, type-specific, could be not easy for local administration. For this reason, efforts should be addressed to obtain combined landslide susceptibility maps, grouping different typologies of phenomena according to geomorphologically adequate criteria. In this sense, a frequently adopted approach is to produce an *a priori* grouped model which means aggregating landslides of more than one typology for calibrating the model. However, generally, these studies do not focus their attention on different behaviours and characteristics of grouped phenomena or, even more, on different the relationships between the geo-environmental predictors and each landslide type.

In this study, an integrated landslide susceptibility map combining flow, slide and complex types is presented for the Visso (Marche, Italy – Main Map, figures a and b) area, which was obtained by combining the final score of the three source independent susceptibility maps. The original landslide inventory was obtained by the reviewing the existing CARG (Geological and Geomorphological Mapping of Italy, Regione Marche 2014) landslide dataset for the 'Visso' map. In facts, mapped single phenomena were often grouped inside large polygons, with a low resolution both in terms of the spatial pattern and typological characterization. For this reason, by exploiting topography maps and orthophotos, the original polygons were split according to the movement typology thus producing separated slides, flows, and complex landslides archives (198, 91, and 51 cases, respectively). By exploiting the LCL_SLU (Martinello et al., 2021, 2022a) as mapping units and Multivariate Adaptive Regression Splines (MARS) statistical method, three specific susceptibility models were prepared by regressing each landslide inventory on a specific set of physical-environmental

CONTACT Margherita Bufalini margherita.bufalini@unicam.it Via Gentile III da Varano, Camerino 62032, Italy

predictors. Furthermore, multicollinearity and variable importance analyses were carried out to verify their relevance and influence in landslide susceptibility assessment. After attesting the sharing of some of the most important variables for the three models, a combined landslide susceptibility map was obtained by adding the three scores of the three single maps. The final integrated map (whose combined score was scaled to a range between 0 and 1) was finally submitted to double validation: the first with respect to the modified CARG archive (putting together slide, flow and complex archives); the second, by exploiting a new inventory obtained by remote checking on Google Earth. The high performance of the model suggests a geomorphologically suitable final map.

2. Data and methods

2.1. Geological, geomorphological and climatic setting

The Umbria-Marche Apennines constitutes the external sector of the central Apennines, a fold-and-thrust belt, NE verging, formed by the convergence between the Corsica-Sardinia and the Adria continental margins. This sector of the Apennines is characterized by arcuated contractional structures (Neogene folds and thrusts faults) involving a Mesozoic-Tertiary sedimentary sequence (Figure 1).

The study area consists of a ~ 30 km^2 sector of the Sibillini Massif, that characterizes the southern portion of the Umbria-Marche Apennines. The geological framework is characterized by the Umbria-Marche succession (Calamita & Deiana, 1988; Pierantoni et al., 2013) composed by a multilayer of pelagic and emipelagic formations, with alternating calcareous, marly calcareous, calcareous-siliceous and siliceous rocks.

The physical landscape is characterized by a predominantly mountainous territory, with reliefs that exceed 1800-2000m a.s.l. (2051m a.s.l. at Mount Bicco). The slopes are often steep, with angles that exceed even 70°, while the valley floors are narrow and strongly incised.

In these conditions the continental deposits (Pleistocene-Holocene in age) are reduced both in extension and in thickness and are mainly made up of slope deposits, sometimes cemented, debris and alluvial fans, and fluvial deposits (Gentili et al., 2017). Gravitational morphogenesis is also very important and represented by rockfalls, slides (both rotational and translational), and flows (mainly debris flows); very frequent are the complex phenomena usually made by slides that evolve downstream in rapid flows (Aringoli et al., 2010; Buccolini et al., 2020; Materazzi et al., 2021) (Figure 2).

From a climatic point of view, the study area is characterized by an Apennine-Adriatic regime with rainfall almost uniformly distributed throughout the year; the highest values are recorded late in autumn and during spring while the lowest ones, in July and January (Gentilucci et al., 2020, 2021). The total annual precipitation often exceeds 1500 mm with 1000 mm isohyet encompassing the whole mountain area. A snowy contribution from November to April is also present; the quantity and persistence of snow increase with the altitude. The study area shows average temperatures of almost 11°C, with a significant increase of 0.5 C in the last 30 years on average, due to climate change (Gentilucci et al., 2019).

2.2. Landslide inventory dataset and diagnostic area

For this study, the data from the landslide inventory of the Marche Region in the year 2000 were initially collected and homogenized, later also used for the editing of the Regional Geological Map at 1: 10,000 scale (Marche Region, 2014). Subsequently, to verify their evolution over time, integration and re-measurement of the landslide areas were carried out using a colour orthophoto of 2020 at the same scale. For the classification of landslides, according to Cruden and Varnes (1996), three main categories (slides, flows, and complex) and four states of activities (new activation, inactive, reactivated, and partly reactivated), were assumed; among these, only one seismic-induced landslide as a consequence of the 2016 central Italy earthquake seismic sequence has been recorded (Aringoli et al., 2021; Farabollini et al., 2018; Romeo et al., 2017;). Fall and topple as well as deep-seated landslide were here excluded as literature generally employs a direct and/or physical-based approach (e.g. Agnesi et al., 2015; Cafiso et al., 2021; Cafiso & Cappadonia, 2019; Cappadonia et al., 2019, 2021; Pappalardo et al., 2021).

According to the inventory review, 351 phenomena (Figure 3) were included, whose summary characteristics are given in Table 1.

The data collected show that the most numerous phenomena fall into the 'slides' category although complex landslides are those that, referring to the single phenomenon, have the greater areal extension. The most elevated landslide density is, instead, that of flows which represent, among other things, almost all the new phenomena (90%) that took place between 2000 and 2020.

The recognized landslides were mapped by using a Landslide Identification Point (LIP), which corresponds to the highest point along the crown of the landslide area here assumed as diagnostic in potentially marking unstable slope conditions (Cama et al., 2015; Lombardo et al., 2014, 2016; Rotigliano et al., 2011, 2018, 2019).

2.3. Mapping units and landslide conditioning factors

According to Martinello et al. (2021, 2022a), the LCL_SLU were used as mapping unit. This type of

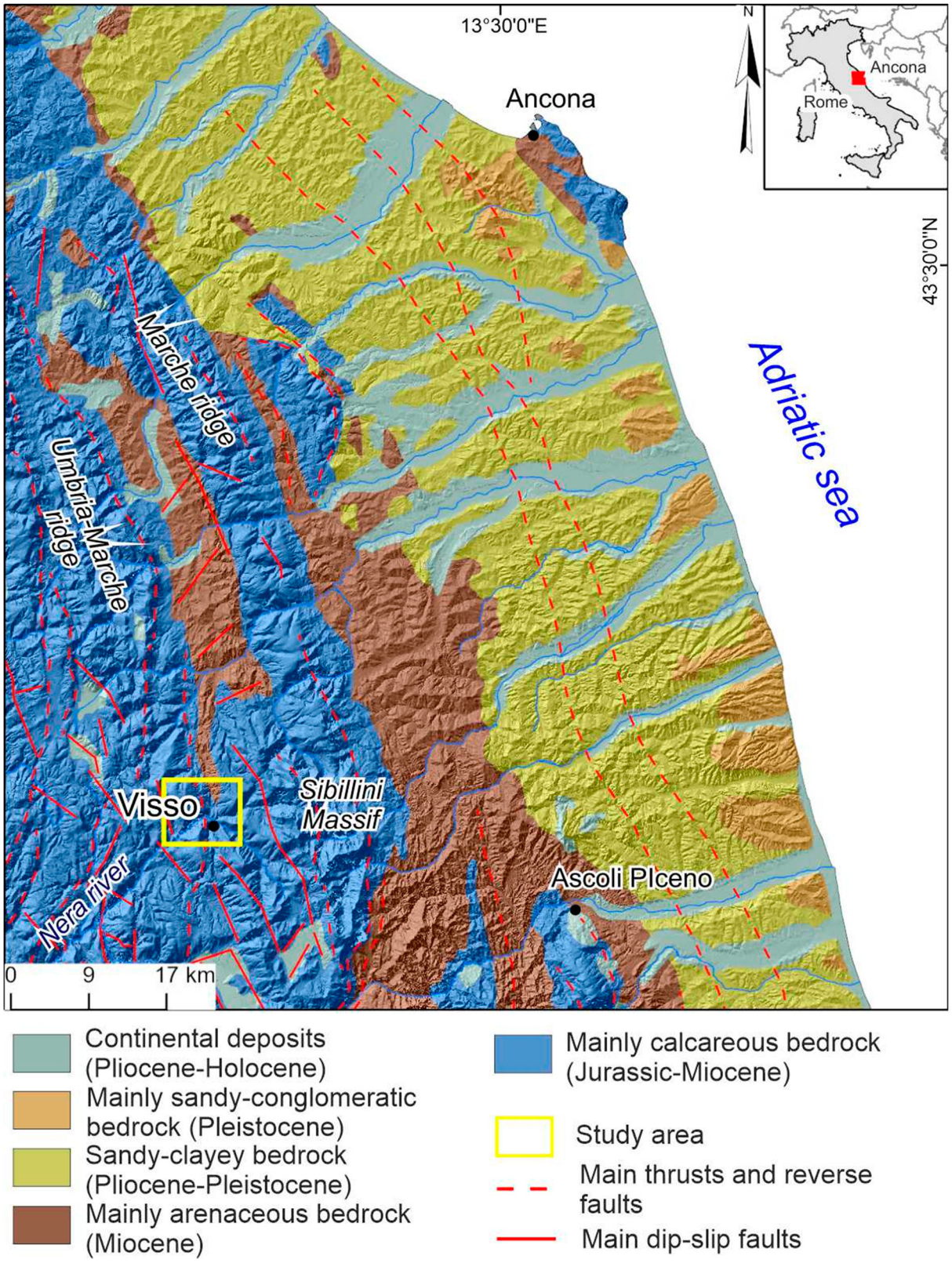

Figure 1. Geological sketch of the study area.

slope unit is obtained by intersecting the classic hydromorphological unit by means of 5000 cells contributing area threshold with the classes of the Landform Classification (LCL; Guisan et al., 1999). The LCL was obtained by exploiting the TPI-based Landform Classification (LCL; Guisan et al., 1999) SAGA tool, by fixing the inner/outer radius as 100/1000 metres. For more information about the LCL_SLU, please refer to the original research of Martinello et al. (2021) and Martinello et al. (2022a).

Each LCL_SLU was then classified as stable or unstable (positive or negative cases) depending on whether it hosts at least one LIP.

Based on the expected direct or proxied role in landsliding (Costanzo et al., 2012; Mercurio et al., 2021; Rotigliano et al., 2018, 2019; Vargas-Cuervo

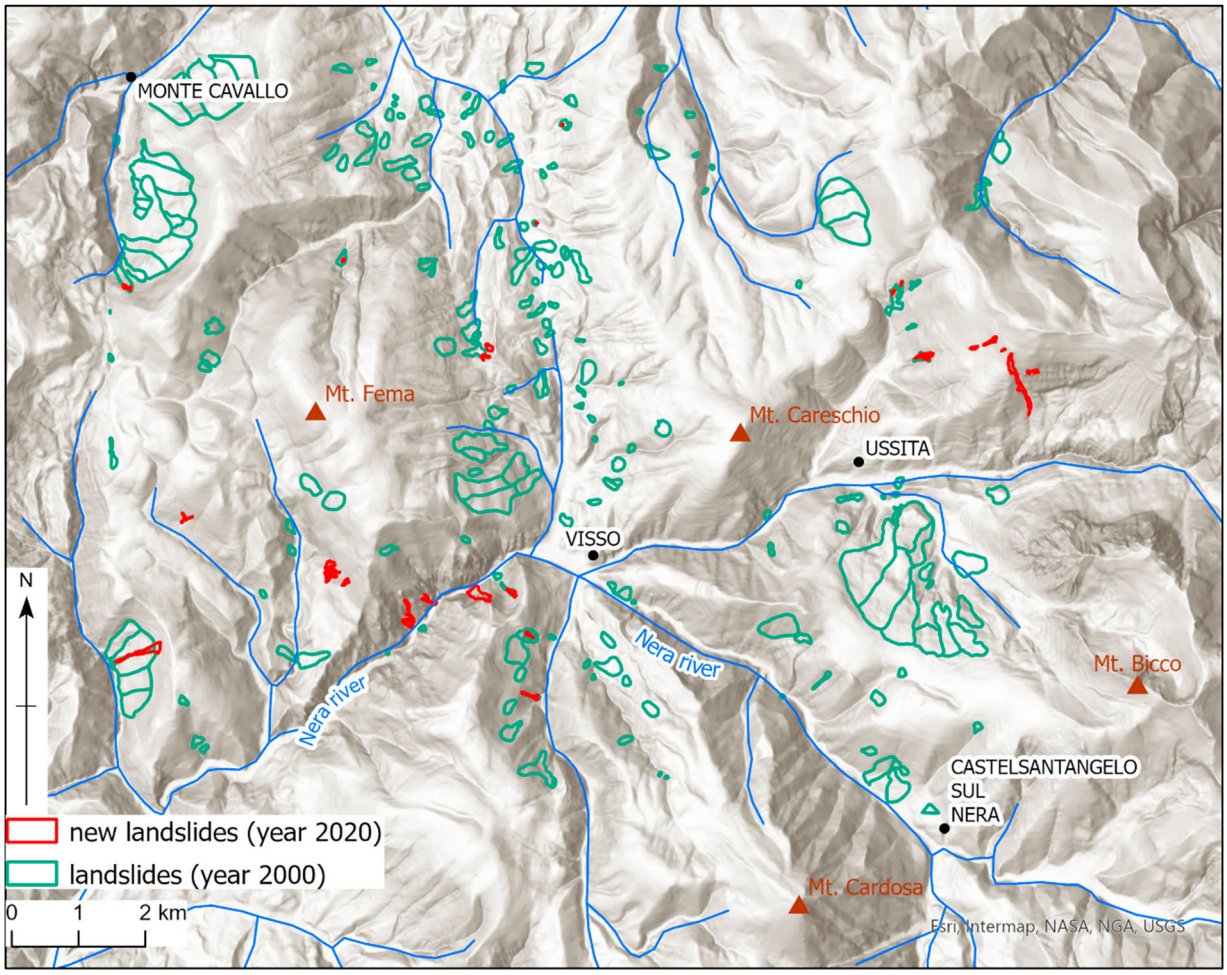

Figure 2. Mountain portion of the Nera River basin: landslide inventory used in the present study.

et al., 2019) eleven geo-environmental factors were considered as potential predictors: outcropping lithology (LITO), land use (obtained by the Corine Land Cover 2000 – USE), elevation (ELE), landform classification (LCL), steepness (SLO), aspect (expressed as Northerness and Easterness), plan (PLN) and profile (PRF) curvatures, topographic wetness index (TWI), and stream power index (SPI). Table 2 gives for each of the selected predictors the main characteristics and the potential proxied significance.

Before starting the modelling procedures, the DEM-derived variables were submitted to multicollinearity analysis, based on the evaluation of the Variance Inflation Factor (VIF) obtained by applying the 'usdm' R-package (Naimi, 2017). All the variables passed the multicollinearity test. According to the specific characteristics of the landslide types analysed in this research, all the predictors were employed for complex type modelling, SPI predictor was excluded for the slide model, while the TWI variable was excluded for the flow model.

To assign the variables to the slope units, the continuous variables were attributed by deciles, while relative frequencies were employed for categorical ones.

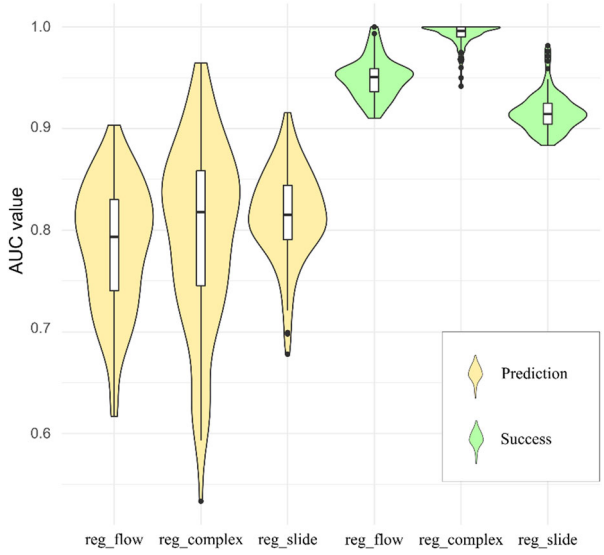

Figure 3. Violin boxplots of the three single models both for prediction and success procedures.

2.4. Statistical model and validation tools

Between the different approaches offered by the literature, several researchers have been exploiting the

Table 1. Summary table of the landslide inventory.

Type of landslide	N. of landslides (year 2000)	N. of landslides (year 2020)	Area involved – year 2000 (km^2)	Landslide density 2000 (n./area)	Area involved – year 2020 (km^2)	Landslide density 2020 (n./area)
Flow	73	100	1.29	56.59	1.35	74.07
Slide	197	199	5.23	37.67	5.23	38.04
Complex	51	52	3.69	13.82	3.69	14.09
Total	321	351	10.21	31.44	10.27	34.17

State of Activity	N. of landslides (year 2020)	Area involved – year 2020 (km^2)
Inactive	312	10.07
New activation	30	0.16
Reactivated	2	0.01
Partly reactivated	7	0.01
Total	351	10.25

Multivariate Adaptive Regression Splines (MARS; Friedman, 1991) method to favourably determine nonlinear relationships and complex interactions in several fields of the science (e.g. Cervantes et al., 2020; Conoscenti et al., 2021). In the last ten years, the MARS method successfully was employed for landslide susceptibility evaluation (e.g. Conoscenti et al., 2015, 2016; Felicísimo et al., 2013; Martinello et al., 2021, 2022a, 2022b; Mercurio et al., 2021; Rotigliano et al., 2018, 2019; Wang et al., 2015), by regressing the outcome (stable/unstable status) onto the covariates set from the controlling factor layers.

MARS is a non-parametric regression method that exploits the splitting of each independent variable into hinge functions to boost the maximum likelihood-based adaptation skill of the logistic regression method, according to

$$y = f(x) = \alpha + \sum_{i=1}^{N} \beta_i h_i(x) \quad (1)$$

where y is the dependent variable (the outcome) predicted by the function $f(x)$, α is the model intercept, and β_i is the coefficient of the h_i basis functions, given the N number of basis functions. By exploiting the 'earth' R-package (Milborrow, 2014), the MARS analysis was performed.

Since this type of statistical modelling relies on a balanced assessment of status cases, a random extraction of negative in the same number of positive cases was carried out. For testing the independence of the result from the selection of negative/positive cases: (1) the extraction of negative cases was replicated one-hundred times and the models' accuracy and precision evaluated (Costanzo et al., 2014; Martinello et al., 2021; Martinello et al., 2022a, 2022b); (2) according to Chung and Fabbri (2003), random splitting procedures were employed to verify the prediction skill of the model by using 75% of the balanced archive for the training phase and the remaining 25% for the validation one.

The performances of the models were evaluated by adopting both cut-off independent and dependent metrics. In particular, the AUC value (Area Under Curve) in the ROC (Receiver Operating Characteristics – Fawcett, 2006; Goodenough et al., 1974; Lasko et al., 2005) was employed to evaluate the prediction skill of the model and to obtain the Youden index optimized cut-off (Youden, 1950). Then, by exploiting the optimized cut-off the true/false positive/negative cases (i.e. TP, TN, FP, and FN, respectively) were distinguished and confusion matrices evaluated.

2.5. Model building and validation strategies

According to the aim of this research, single models for each type of landslide were first prepared by using the three 2000 inventories. In this way, three source models and related landslide susceptibility maps were prepared and validated: reg_slide, reg_flow and reg_complex, for slide, flow and complex landslides, respectively. A combined map was then obtained by adding the three source scores and re-scaling the combined value on the 0–1 range. Finally, the prediction skill of the combined map was tested in detecting both all the 2000 landslides and, according to a temporal partition, the unknown 2020 phenomena.

3. Results

In Figure 3 the boxplot for the three single models reg_slide, reg_flow and reg_complex, both for the validation to the blinded 25% (prediction) and the success validations are reported. In particular, based on replicates we produced through multiple random positive/negative extraction, the distribution of the one-hundred AUC values is plot, so to estimate accuracy and precision of each of the three models. The results attest good and excellent (Hosmer & Lemeshow, 2000) AUC mean values for the prediction (0.78, 0.81 and 0.8, respectively for reg_flow, reg_slide and reg_complex). However, medium standard deviations are associated with these AUC mean values (from 0.05 to 0.09).

Table 2. Details of the employed geo-environmental variables (modified from Martinello et al., 2022b).

Factor	Acronym	Description of predictor	Units	References	Potential proxy signifiance
Elevation	ELE	distribution of elevation	m	Tinitaly (Tarquini et al., 2007)	Mean annual rainfall
Landform classification	LCL	morphological classification of the territory based on the variation in elevation with respect to the neighbouring areas		Guisan et al. (1999)	Morphological setting
Steepness	SLO	the first derivative of elevation	degree	Burrough and McDonnell (1998)	Speed of the water and potential underlying rupture surfaces (Martinello et al., 2022a)
Northerness	N	cosine of aspect (direction in which the slope degrades more rapidly)		Wilson and Gallant (2000)	Seasonal wet/dry cycles of soils (Auslander et al. 2003)
Easterness	E	sine of aspect (direction in which the slope degrades more rapidly)		Wilson and Gallant (2000)	Seasonal wet/dry cycles of soils (Auslander et al. 2003)
Plan curvature	PLN	The second derivative of elevation, computed along the horizontal plane	rad/m	Zevenbergen and Thorne (1987)	Activation and propagation of landslides (Ohlmacher, 2007)
Profile curvature	PRF	The second derivative of elevation, computed along the direction of the highest slope gradient	rad/m	Zevenbergen and Thorne (1987)	The direction of flow (Ohlmacher, 2007)
Topographic wetness index	TWI	Calculated as ln[A/tanβ], where A and β, computed on each cell, corresponds to the area of upslope drained cells and the slope gradient, respectively	m	Beven and Kirkby (1979)	Potential infiltration or saturated soil thickness (Martinello et al., 2022a; Rotigliano et al., 2011)
Stream Power Index	SPI	natural logarithm of the catchment area multiplicated the tangent of the slope gradient		Florinsky (2012)	Proxy of the intensity of surface water erosion (Martinello et al., 2022a)
Lithological map	LITO	original geological map		Marche Region (2014)	Physical-mechanical properties of rocks (Martinello et al., 2022a)
Soil use	USE	CORINE land cover (2000)		Büttner et al. (2000)	Potential hydrological and surface hydric erosion induced disturbances (Martinello et al., 2022a)

Better performances are obtained from success models, with outstanding AUC mean values (0.95, 0.92 and 0.99, respectively for reg_flow, reg_slide and reg_complex) and very low standard deviations of replicates (from 0.01 to 0.02).

High performances are also revealed by the confusion matrices (Table 3) both for prediction and success validation. For the latter, the increase in the performances is more marked, especially for the complex type model. The sensitivity for the prediction validation is just below 0.8 while the values increase for success validations ranking from 0.82 to 0.97. Similar behaviour is reported for the specificity which attests around 0.7 for the prediction validations, increasing up to 0.97 in success validations.

Table 4 shows the 10 most important variables for the reg_flow, reg_slide and reg_complex success models. It is important to note that this type of analysis highlights only how frequently the class of the variables is employed for the construction of the model. Therefore, the analysis shows if a class of the variable is used to discriminate positive to negative cases by the model, but it is not diriment for defining if the class is positively or negatively correlated with landsliding. In this sense, the old landslide deposits class (lito12) is a very important class for all types of models considering that its overall ranks from 95 to 100 (even employed for the model construction). The max value of the elevation is a very important class of variable for reg_complex and reg_flow models. These models also share the natural grassland class of USE as important. The second most important class for reg_slide, the max value of PRF, is also the 5th for reg_flow while the Q100 of PLC, in common between reg_slide and reg_complex, is recalled around 10 times.

In figure c of the main map, the combined landslide susceptibility map for the Visso area is proposed. The four different landslide susceptibility classes are defined by employing nested Youden index cut-offs (low = 0.25, mean = 0.39, high = 0.61). For a more manageable definition of susceptibility, the ranges are linked to nominal classes described as S1 or 'low', S2 or 'moderate', S3 or 'High' and S4 or 'Very High' susceptibility levels.

The validation of the final map with respect to the 2000 inventory shows good performances with an AUC value of 0.87 (Figure 4(a)) and a very high

Table 3. Confusion matrix of the three single models both for prediction and success procedures.

	Model	Cut-off	TN	FN	FP	TP	Acc.	Sens.	Spec.
Prediction	reg_flow	0.42	21	7	9	23	0.73	0.77	0.69
	reg_slide	0.46	41	13	17	45	0.74	0.77	0.71
	reg_complex	0.11	11	3	4	12	0.75	0.79	0.71
Success	reg_flow	0.5	107	13	15	109	0.88	0.89	0.88
	reg_slide	0.46	191	33	43	201	0.86	0.82	0.84
	reg_complex	0.47	58	1	2	59	0.98	0.97	0.97

Table 4. Most important variables for the three main models.

reg_flow		reg_slide		reg_complex	
variable	mean	variable	mean	variable	mean
lito12	100	lito12	98	lito12	95
lito5	52	prf[q100]	56	ele[q100]	42
ele[q100]	48	lito18	44	lcl0	17
lito9	29	lcl0	27	E[q20]	15
prf[q100]	23	lcl5	23	use7	15
ele[q10]	18	slo[q60]	21	ele[q90]	13
use10	12	prf[q10]	16	ele[q80]	13
lito19	12	plc[q100]	12	use10	12
use8	11	N[q100]	11	N[q90]	8
lcl0	10	slo[q80]	11	plc[q100]	7

In red, the predictors are employed by all three models: in light blue, by only two models. Legend: lito12 = old landslide deposits; lito5 = clayey marls, lito9 = calcareous units, lito19 = 'scaglia cinerea' clays, lito18 = 'scaglia bianca' clays, corine10 = natural grassland, corine8 = coniferous forest, corine7 = broad-leaved forest, lcl0 = streams, lcl5 = open slopes.

value of sensitivity (0.87) and good specificity (0.78). At the same time, the comparison with the 2020 inventory confirms a generally good quality of the final map despite a slight lowering of the performance, with an AUC value of 0.84 and 0.79 e 0.72 for sensitivity and specificity, respectively. In Figure 4(b) the degree of fit for the landslides of 2000 and 2020 is shown. It is worth noting that more than 80% of landslides are correctly classified both with respect to the 2000 archive and the 2020 ones (87% and 80% respectively). Only 5% of the 2000 inventory (4% for the 2020 inventory) is incorrectly classified by the map in the low susceptibility class, while 8% (15% for the 2020 inventory) is allocated in the moderate class.

4. Discussion and conclusion

Excellent performances result for the three single models (reg_flow, reg_slide, reg_flow), both in prediction validation and in the success tests. The violin plots show a larger but limited (std. dev. < 0.1) dispersion of the AUC values for the prediction analysis. On the other hand, excellent and stable AUC values were obtained in success analysis. These high performances were confirmed also by the cut-off dependent matrices. The analysis of the importance of the variables suggested lito12 ('old landslide deposits') is the more employed class for the construction of the models, for all the typologies investigated. This suggests that most of the landslides of the 2000 inventory (that correspond to the calibration archive) are a reactivation of old phenomena. The comparison shows also that other variables or classes of predictors are in common between the three models: prf (max value), ele (max value) plc (max value) and use10. On the other hand, some classes of geo-environmental predictors are essential only for single specific models: lito5 (clayey marls) is important for flow type, lito18 ('scaglia bianca' clays) for slides while more use of dem-derived variables resulted for complex type. These behaviours encourage the grouping of the three types of landslides, suggesting also that grouping in the calibration phase could have hidden some of the relationships between a specific movement and its related geo-environmental predictors. On the contrary, by adding together the susceptibility score obtained by the single modelling procedures, the specificity of each model and, in this way, the peculiarity of landslide typology can be noticed. At the same time, the combined landslide map showed high performances in validation both with respect to the 2000 and the unknown 2020 inventories. For the latter, it is worth noting a slight lowering of the performances. According to the analysis of the variable's importance, the models are more sensitive to reactivation movements. Considering the characteristics of the two landslide inventories, this lowering could be linked to the state of activity of the phenomena: with

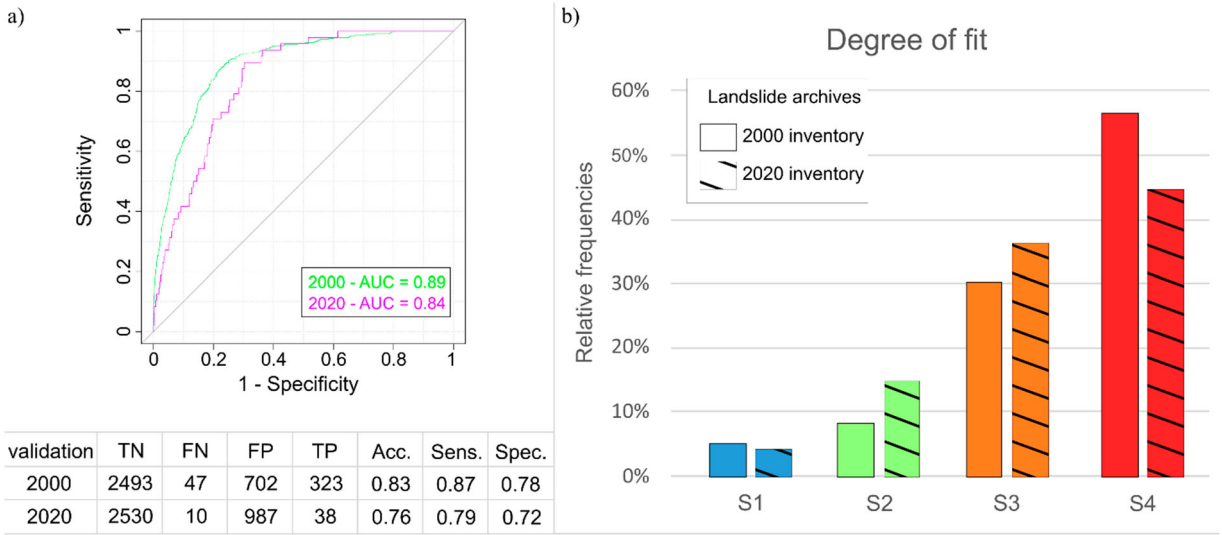

validation	TN	FN	FP	TP	Acc.	Sens.	Spec.
2000	2493	47	702	323	0.83	0.87	0.78
2020	2530	10	987	38	0.76	0.79	0.72

Figure 4. Validation indices of the combined map for the validation with respect to the 2000 inventory and the 2020 one. (a) ROC-curves and AUC values and, in the bottom, confusion matrices; (b) degree of fit plot.

respect to the 2020 year, the most of 2000 landslides are in facts still dormant.

The results obtained in this application on the Visso area allow us to consider the approach employed for producing a combined landslide susceptibility map for the flow, slide and complex landslide types as geomorphological suitable.

Software

The landslides were remotely verified and remapped by using Google Earth Pro. In the first step for the production of LCL_SLU, GRASS GIS (GRASS Development Team, 2022) was utilized to obtain the SLU by using the r.watershed processing. In the second step, Saga GIS 8.0.0 (Conrad et al., 2015) was employed to produce the LCL map and to clip the SLUs with the LCL map. Saga GIS 8.0.0 was also employed to obtain the dem-derived variables and to rasterize the variables available in.shp format. Quantum GIS3.8.2 Zanzibar (QGIS.org, 2022)was used to print all maps displayed in this research. The models were implemented by using the RStudio (RStudio Team, 2020) software.

Disclosure statement

No potential conflict of interest was reported by the author (s).

Data availability statement

All authors agree to share the data and materials that support the results and the analyses freely available upon request. The sharing does not violate the protection of human subjects, or other valid ethical, privacy, or security concerns.

ORCID

Chiara Martinello http://orcid.org/0000-0001-9527-487X
Margherita Bufalini http://orcid.org/0000-0003-3278-7058
Chiara Cappadonia http://orcid.org/0000-0002-5119-3004
Edoardo Rotigliano http://orcid.org/0000-0002-1072-3160
Marco Materazzi http://orcid.org/0000-0002-9480-5680

References

Agnesi, V., Rotigliano, E., Tammaro, U., Cappadonia, C., Conoscenti, C., Obrizzo, F., Maggio, C. D., Luzio, D., & Pingue, F. (2015). GPS monitoring of the Scopello (Sicily, Italy) DGSD phenomenon: Relationships between surficial and deep-seated morphodynamics. In *Engineering geology for society and territory-Volume 2: Landslide processes* (pp. 1321–1325). Springer International Publishing. https://doi.org/10.1007/978-3-319-09057-3_232

Aringoli, D., Farabollini, P., Pambianchi, G., Materazzi, M., Bufalini, M., Fuffa, E., & Scalella, G. (2021). Geomorphological hazard in active tectonics area: Study cases from Sibillini Mountains thrust system (Central Apennines). *Land*, *10*(5), 510. https://doi.org/10.3390/land10050510

Aringoli, D., Gentili, B., Materazzi, M., & Pambianchi, G. (2010). Mass movements in Adriatic Central Italy: Activation and evolutive control factors. In E. D. Werner, & H. P. Friedman (Eds.), *Landslides: causes, types and effects* (pp. 1–71) New York, NY: Nova Science Publisher, Inc.

Beven, K. J., & Kirkby, M. J. (1979). A physically based, variable contributing area model of basin hydrology. *Hydrological Sciences Bulletin*, *24*(1), 43–69. https://doi.org/10.1080/02626667909491834

Buccolini, M., Bufalini, M., Coco, L., Materazzi, M., & Piacentini, T. (2020). Small catchments evolution on clayey hilly landscapes in Central Apennines and northern Sicily (Italy) since the Late Pleistocene. *Geomorphology*, *363*, 107206. https://doi.org/10.1016/j.geomorph.2020.107206

Bufalini, M., Materazzi, M., De Amicis, M., & Pambianchi, G. (2021). From traditional to modern 'full coverage' geomorphological mapping: A study case in the Chienti river basin (Marche region, central Italy). *Journal of Maps*, *17*(3), 17–28. https://doi.org/10.1080/17445647.2021.1904020

Büttner, G., Feranec, J., Jaffrain, G., Steenmans, C., Gheorghe, A., & Lima, V. (2002). *Corine land cover update 2000*. Technical guidelines.

Burrough, P. A., & McDonnell, R. A. (1998). Principle of geographic information systems CODRA-creating opportunities to develop resilient agriculture view project groundwater governance in the Arab world: Taking stock and addressing the challenges view project. https://www.researchgate.net/publication/37419765

Cafiso, F., & Cappadonia, C. (2019). Landslide inventory and rockfall risk assessment of a strategic urban area (Palermo, Sicily). *Rendiconti Online Societa Geologica Italiana*, *48*, 96–105. https://doi.org/10.3301/ROL.2019.42

Cafiso, F., Cappadonia, C., Ferraro, R., & Martinello, C. (2021). Rockfall hazard assessment of the Monte Gallo Oriented Nature Reserve area (Southern Italy). *IOP Conference Series: Earth and Environmental Science*, *833* (1), 1. https://doi.org/10.1088/1755-1315/833/1/012176

Calamita, F., & Deiana, G. (1988). The arcuate shape of the Umbria-Marche-Sabina Apennines (central Italy). *Tectonophysics*, *146*(1-4), 139–147. https://doi.org/10.1016/0040-1951(88)90087-X

Cama, M., Lombardo, L., Conoscenti, C., Agnesi, V., & Rotigliano, E. (2015). Predicting storm-triggered debris flow events: Application to the 2009 Ionian Peloritan disaster (Sicily, Italy). *Natural Hazards and Earth System Sciences*, *15*(8), 1785–1806. https://doi.org/10.5194/nhess-15-1785-2015

Cappadonia, C., Cafiso, F., Ferraro, R., Martinello, C., & Rotigliano, E. (2021). Rockfall hazards of Mount Pellegrino area (Sicily, Southern Italy). *Journal of Maps*, *17*(3), 29–39. https://doi.org/10.1080/17445647.2020.1824826

Cappadonia, C., Confuorto, P., Sepe, C., & di Martire, D. (2019). Preliminary results of a geomorphological and DInSAR characterization of a recently identified deep-seated gravitational slope deformation in Sicily (Southern Italy). *Rendiconti Online Societa Geologica*

Italiana, *49*, 149–156. https://doi.org/10.3301/ROL.2019.65

Cervantes, P. A. M., López, N. R., & Rambaud, S. C. (2020). The relative importance of globalization and public expenditure on life expectancy in Europe: An approach based on mars methodology. *International Journal of Environmental Research and Public Health*, *17*(22), 1–20. https://doi.org/10.3390/ijerph17228614

Chung, C.-J.-F., & Fabbri, A. G. (2003). Validation of spatial prediction models for landslide hazard mapping. *Natural Hazards*, *30*(3), 451–472. https://doi.org/10.1023/B:NHAZ.0000007172.62651.2b

Conoscenti, C., Ciaccio, M., Caraballo-Arias, N. A., Gómez-Gutiérrez, T., Rotigliano, E., & Agnesi, V. (2015). Assessment of susceptibility to earth-flow landslide using logistic regression and multivariate adaptive regression splines: A case of the Belice River basin (western Sicily, Italy). *Geomorphology*, *242*, 49–64. https://doi.org/10.1016/j.geomorph.2014.09.020

Conoscenti, C., Martinello, C., Alfonso-Torreño, A., & Gómez-Gutiérrez, Á. (2021). Predicting sediment deposition rate in check-dams using machine learning techniques and high-resolution DEMs. *Environmental Earth Sciences*, *80*(10), 1–19. https://doi.org/10.1007/s12665-021-09695-3

Conoscenti, C., Rotigliano, E., Cama, M., Caraballo-Arias, N. A., Lombardo, L., & Agnesi, V. (2016). Exploring the effect of absence selection on landslide susceptibility models: A case study in Sicily, Italy. *Geomorphology*, *261*, 222–235. https://doi.org/10.1016/j.geomorph.2016.03.006

Conrad, O., Bechtel, B., Bock, M., Dietrich, H., Fischer, E., Gerlitz, L., Wehberg, J., Wichmann, V., & Böhner, J. (2015). System for automated geoscientific analyses (SAGA) v. 2.1.4. *Geoscientific Model Development*, *8*(7), 1991–2007. https://doi.org/10.5194/gmd-8-1991-2015

Costanzo, D., Chacón, J., Conoscenti, C., Irigaray, C., & Rotigliano, E. (2014). Forward logistic regression for earth-flow landslide susceptibility assessment in the Platani river basin (southern Sicily, Italy). *Landslides*, *11*(4), 639–653. https://doi.org/10.1007/s10346-013-0415-3

Costanzo, D., Rotigliano, E., Irigaray, C., Jiménez-Perálvarez, J. D., & Chacón, J. (2012). Factors selection in landslide susceptibility modelling on large scale following the gis matrix method: Application to the river Beiro basin (Spain). *Natural Hazards and Earth System Science*, *12*(2), 327–340. https://doi.org/10.5194/nhess-12-327-2012

Cruden, D. M., & Varnes, D. J. (1996). Landslide types and processes. Special Report National Research Council Transportation Research Board. *National Academy of Sciences*, *247*, 36–75.

Farabollini, P., Angelini, S., Fazzini, M., Lugeri, F. R., & Scalella, G. (2018). La sequenza sismica dell'Italia centrale del 24 agosto e successive: Contributi alla conoscenza e la banca dati degli effetti di superficie. *Rendiconti Online Della Società Geologica Italiana*, *46*, 9–15. https://doi.org/10.3301/ROL.2018.45

Fawcett, T. (2006). An introduction to ROC analysis. *Pattern Recognition Letters*, *27*(8), 861–874. https://doi.org/10.1016/j.patrec.2005.10.010

Felicísimo, ÁM, Cuartero, A., Remondo, J., & Quirós, E. (2013). Mapping landslide susceptibility with logistic regression, multiple adaptive regression splines, classification and regression trees, and maximum entropy methods: A comparative study. *Landslides*, *10*(2), 175–189. https://doi.org/10.1007/s10346-012-0320-1

Florinsky, I. V. (2012). *Digital terrain analysis in soil science and geology*.

Friedman, J. H. (1991). Multivariate adaptive regression splines. *The Annals of Statistics*, *19*(1), 1–67. http://www.jstor.org/stable/2241837

Gentili, B., Pambianchi, G., Aringoli, D., Materazzi, M., & Giacopetti, M. (2017). Pliocene-Pleistocene geomorphological evolution of the Adriatic side of central Italy. *Geologica Carpathica*, *68*(1), 6. https://doi.org/10.1515/geoca-2017-0001

Gentilucci, M., Barbieri, M., D'Aprile, F., & Zardi, D. (2020). Analysis of extreme precipitation indices in the Marche region (central Italy), combined with the assessment of energy implications and hydrogeological risk. *Energy Reports*, *6*, 804–810. https://doi.org/10.1016/j.egyr.2019.11.006

Gentilucci, M., Bufalini, M., D'Aprile, F., Materazzi, M., & Pambianchi, G. (2021). Comparison of data from rain gauges and the IMERG product to analyse precipitation in mountain areas of central Italy. *ISPRS International Journal of Geo-Information*, *10*(12), 795. https://doi.org/10.3390/ijgi10120795

Gentilucci, M., Materazzi, M., Pambianchi, G., Burt, P., & Guerriero, G. (2019). Assessment of variations in the temperature-rainfall trend in the province of Macerata (Central Italy), comparing the last three climatological standard normals (1961–1990; 1971–2000; 1981–2010) for biosustainability studies. *Environmental Processes*, *6*(2), 391–412. https://doi.org/10.1007/s40710-019-00369-8

Goodenough, D. J., Rossmann, K., & Lusted, L. B. (1974). *Radiographic applications of receiver operating characteristic (ROC) curves l diagnostic radiology*.

GRASS Development Team. (2022). Geographic Resources Analysis Support System (GRASS) software, Version 8.0. In Open Source Geospatial Foundation. . https://grass.osgeo.org

Guisan, A., Weiss, S. B., & Weiss, A. D. (1999). GLM versus CCA spatial modeling of plant species distribution. *Plant Ecology*, *143*(1), 107–122. https://link.springer.com/article/10.1023a:1009841519580 https://doi.org/10.1023/A:1009841519580

Hungr, O., Leroueil, S., & Picarelli, L. (2014). The Varnes classification of landslide types, an update. *Landslides*, *11*, 167–194.

Hosmer Jr., D. W., & Lemeshow, S. (2000). *Applied logistic regression*. 2nd Edition. New York: John Wiley & Sons, Inc. http://dx.doi.org/10.1002/0471722146

Lasko, T. A., Bhagwat, J. G., Zou, K. H., & Ohno-Machado, L. (2005). The use of receiver operating characteristic curves in biomedical informatics. *Journal of Biomedical Informatics*, *38*(5), 404–415. https://doi.org/10.1016/j.jbi.2005.02.008

Lombardo, L., Bachofer, F., Cama, M., Märker, M., & Rotigliano, E. (2016). Exploiting maximum entropy method and ASTER data for assessing debris flow and debris slide susceptibility for the Giampilieri catchment (north-eastern Sicily, Italy). *Earth Surface Processes and Landforms*, *41*(12), 1776–1789. https://doi.org/10.1002/esp.3998

Lombardo, L., Cama, M., Maerker, M., & Rotigliano, E. (2014). A test of transferability for landslides susceptibility models under extreme climatic events: Application to the Messina 2009 disaster. *Natural Hazards*, *74*(3), 1951–1989. https://doi.org/10.1007/s11069-014-1285-2

Martinello, C., Cappadonia, C., Conoscenti, C., Agnesi, V., & Rotigliano, E. (2021). *Optimal slope units partitioning*

in landslide susceptibility mapping. https://doi.org/10.1080/17445647.2020.1805807

Martinello, C., Cappadonia, C., Conoscenti, C., & Rotigliano, E. (2022a). Landform classification: A high-performing mapping unit partitioning tool for landslide susceptibility assessment – A test in the Imera River basin (northern Sicily, Italy). *Landslides*, *19*(3), 539–553. https://doi.org/10.1007/s10346-021-01781-8

Martinello, C., Mercurio, C., Cappadonia, C., Hernández Martínez, MÁ, Reyes Martínez, M. E., Rivera Ayala, J. Y., Conoscenti, C., & Rotigliano, E. (2022b). Investigating limits in exploiting assembled landslide inventories for calibrating regional susceptibility models: A test in volcanic areas of El Salvador. *Applied Sciences (Switzerland)*, *12*(12), 6151. https://doi.org/10.3390/app12126151

Materazzi, M., Bufalini, M., Gentilucci, M., Pambianchi, G., Aringoli, D., & Farabollini, P. (2021). Landslide hazard assessment in a monoclinal setting (Central Italy): Numerical vs. geomorphological approach. *Land*, *10*(6), 624. https://doi.org/10.3390/land10060624

Mercurio, C., Martinello, C., Rotigliano, E., Argueta-Platero, A. A., Reyes-Martínez, M. E., Rivera-Ayala, J. Y., & Conoscenti, C. (2021). Mapping susceptibility to debris flows triggered by tropical storms: A case study of the San Vicente Volcano Area (El Salvador, CA). *Earth*, *2*(1), 66–85. https://doi.org/10.3390/earth2010005

Milborrow, S. (2014). *Notes on the earth package* (pp. 1–60).

Naimi, B. (2017). Package "usdm". Uncertainty analysis for species distribution models. *R-Cran*, 18. https://cran.r-project.org/web/packages/usdm/usdm.pdf

Ohlmacher, G. C. (2007). Plan curvature and landslide probability in regions dominated by earth flows and earth slides. *Engineering Geology*, *91*(2–4), 117–134. https://doi.org/10.1016/j.enggeo.2007.01.005

Pappalardo, G., Mineo, S., Cappadonia, C., Martire, D. D., Calcaterra, D., Tammaro, U., Rotigliano, E., & Agnesi, V. (2021). A combined GNSS-DINSAR-IRT study for the characterization of a deep-seated gravitational slope deformation. *Italian Journal of Engineering Geology and Environment, SpecialIss*, *1*, 151–162. https://doi.org/10.4408/IJEGE.2021-01.S-14

Pierantoni, P., Deiana, G., & Galdenzi, S. (2013). Stratigraphic and structural features of the Sibillini mountains (Umbria-Marche Apennines, Italy). *Italian Journal of Geosciences*, *132*(3), 497–520. https://doi.org/10.3301/IJG.2013.08

QGIS.org. (2022). *QGIS geographic information system*. QGIS Association. http://www.qgis.org

Romeo, S., Di Matteo, L., Melelli, L., Cencetti, C., Dragoni, W., & Fredduzzi, A. (2017). Seismic-induced rockfalls and landslide dam following the October 30, 2016 earthquake in Central Italy. *Landslides*, *14*(4), 1457–1465. https://doi.org/10.1007/s10346-017-0841-8

Rotigliano, E., Agnesi, V., Cappadonia, C., & Conoscenti, C. (2011). The role of the diagnostic areas in the assessment of landslide susceptibility models: A test in the sicilian chain. *Natural Hazards*, *58*(3), 981–999. https://doi.org/10.1007/s11069-010-9708-1

Rotigliano, E., Martinello, C., Agnesi, V., & Conoscenti, C. (2018). Evaluation of debris flow susceptibility in El Salvador (CA): a comparison between Multivariate Adaptive Regression Splines (MARS) and Binary Logistic Regression (BLR). *Hungarian Geographical Bulletin*, *67*(4), 361–373. https://doi.org/10.15201/hungeobull.67.4.5

Rotigliano, E., Martinello, C., Hernandéz, M. A. A., Agnesi, V., & Conoscenti, C. (2019). Predicting the landslides triggered by the 2009 96E/Ida tropical storms in the Ilopango caldera area (El Salvador, CA): optimizing MARS-based model building and validation strategies. *Environmental Earth Sciences*, *78*(6), https://doi.org/10.1007/s12665-019-8214-3

RStudio Team. (2020). *RStudio: Integrated development for R*. RStudio, PBC. http://www.rstudio.com/

Smith, M. J., Paron, P., & Griffiths, J. S. (2011). Geomorphological mapping: Methods and applications. In M. J. Smith, P. Paron, & J. S. Griffiths (Eds.), *Developments in Earth surface processes, vol. 15* (pp. 661), British society for geomorphology.

Tarquini, S., Isola, I., Favalli, M., & Battistini, A. (2007). *TINITALY, a digital elevation model of Italy with a 10 meters cell size* (Version 1.0) [Data set]. Istituto Nazionale di Geofisica e Vulcanologia (INGV).

Vargas-Cuervo, G., Rotigliano, E., & Conoscenti, C. (2019). Prediction of debris-avalanches and -flows triggered by a tropical storm by using a stochastic approach: An application to the events occurred in Mocoa (Colombia) on 1 April 2017. *Geomorphology*, *339*(1999), 31–43. https://doi.org/10.1016/j.geomorph.2019.04.023

Wang, L. J., Guo, M., Sawada, K., Lin, J., & Zhang, J. (2015). Landslide susceptibility mapping in Mizunami City, Japan: A comparison between logistic regression, bivariate statistical analysis and multivariate adaptive regression spline models. *Catena*, *135*, 271–282. https://doi.org/10.1016/j.catena.2015.08.007

Wilson, J. P., & Gallant, J. C. (2000). Primary topographic attributes. In J. P. Wilson, & J. C. Gallant (Eds.), *Terrain analysis: Principles and applications* (p. 426). John Wiley & Sons.

Youden, W. J. (1950). Index for rating diagnostic tests. *Cancer*, *3*(1), 32–35. https://doi.org/10.1002/1097-0142(1950)3:1<32::AID-CNCR2820030106>3.0.CO;2-3

Zevenbergen, L. W., & Thorne, C. R. (1987). Quantitative analysis of land surface topography. *Earth Surface Processes and Landforms*, *12*(1), 47–56. https://doi.org/10.1002/esp.3290120107